Available online at www.sciencedirect.com
ScienceDirect
Computational Materials Science 38 (2006) 67–74
COMPUTATIONAL MATERIALS SCIENCE
www.elsevier.com/locate/commatsci

Network model of fluid flow in semi-solid aluminum alloys

W.O. Dijkstra [a], C. Vuik [b], L. Katgerman [a,*]

[a] Department of Materials Science, Delft University of Technology, Rotterdamseweg 137, 2628 AL Delft, Netherlands
[b] Department of Applied Mathematical Analysis, Delft University of Technology, Mekelweg 4, 2628 CD Delft, Netherlands

Received 15 June 2005; received in revised form 3 January 2006; accepted 9 January 2006

Abstract

A network model is presented to simulate solidification and fluid flow within a semi-solid aluminum alloy. The model consists of a set of connected channels representing the interdendritic liquid and its possible flow directions at high solid fractions (>0.7). The individual channels react according to solidification rules upon liquid solute convection and changes of the local temperature. This dynamic network model has been designed in such a way that a qualitative study of the interaction between the channels is possible. The simulations of the alloys considered show good agreement with the expected macroscopic fluid flow behavior. The simulations indicate a possible reason for deviations from the Kozeny–Carman relationship in measurements of semi-solid alloys.

PACS: 02.70.Rw; 47.11.+j; 47.55.Mh; 81.05.Bx; 81.05.Rm; 81.30.Fb

Keywords: Network modeling; Simulation; Fluid flow; Aluminum alloys; Permeability; Macrosegregation

1. Introduction

Early simulations of the solidification of alloys often used an averaging approach [1]. This approach describes all physical properties within a representative volume element (REV) in terms of fraction solid or liquid. Even though the approach has had many refinements and extensions [2–6] its principles are still used today to simulate solidification on a macroscopic level (e.g. [5]). Since the early simulations however the uncertainty remains of how to determine the fluid flow rate within a semi-solid REV given the pressure on its boundary. With few exceptions averaged based simulations have assumed that Darcy's law is applicable. According to Darcy's law the fluid flow rate is proportional to the applied pressure difference [7].

The problem which arises is to find an adequate proportionality constant, i.e. to determine permeability. An obvious way to do this is to measure it using an alloy or a similar substance. This has been done many times with various experimental settings e.g. [8–12]. Apart from the obvious difficulty that the underlying micro-structure of the semi-solid might vary during the experiment, a number of additional limitations of the experiments have been described [19]. Furthermore, the measurements show a rather wide spread, which makes it difficult to fit them to a general rule relating permeability to the fraction of solid (or liquid) [20,21]. However, most experiments report however good agreement with the Kozeny–Carman relationship (1), at least within a certain range of liquid or solid fractions (about $0.5 < f_s < 0.9$ in [19]) and with the right (individual) fitting parameters.

The Kozeny–Carman relationship is given by

$$K = \frac{f_l^3}{k_c S_S^2}, \tag{1}$$

where K is the permeability, f_l is the volume fraction of liquid, S_S is the solid–liquid interfacial area per unit volume and k_c is the Kozeny constant. This equation can directly be derived from the assumption that the whole

* Corresponding author. Tel.: +31 15 278 2249; fax: +31 15 278 6730.
E-mail address: l.katgerman@tnw.tudelft.nl (L. Katgerman).

0927-0256/$ - see front matter © 2006 Elsevier B.V. All rights reserved.
doi:10.1016/j.commatsci.2006.01.007

porous and semi-solid alloy (or other porous media) can be represented by a set of straight and parallel tubes. This rather crude approximation shows, for many sorts of porous media, a remarkably good agreement with reality as long as the Kozeny constant can be estimated [22–24].

The Kozeny constant can be expected to vary generally most at high and very low liquid fractions [25]. For very low liquid fractions the known experiments using semi-solid alloys seem not to be very suitable. Therefore, it is not surprising that fluid flow has been numerically simulated using micro-photographs of the structure of quenched alloys [26–31]. This technique ignores completely the dynamic changes of the micro-structure and there are some uncertainties on how the quenching process affects the micro-structure. Until now, there remains some doubts about the applicability of the Kozeny–Carman relationship and the correct value of the Kozeny constant [32].

Another approach to describe permeability was adapted by Wang and Beckermann [33–37]. The main idea behind the derived equation is that the dendritic micro-structure of the semi-solid can be represented by a set of spheres. Through the distinction of intra- and inter-spheric liquid, detailed description of fluid flow and solidification becomes possible. New measurements show that the expression established by these authors and the Kozeny–Carman relationship do not deviate significantly over a wide range of liquid fractions [12].

The fluid flow within solidifying alloys has been studied in various other works. Among them, theoretical considerations including closure problems are used in [13–15]. More detailed (micro-)structures were simulated applying the phase-field method [16–18]. None of them however made any conclusive remarks about the usability of the Kozeny–Carman relationship.

For this purpose a cellular automata model which seems to have been restricted to a small 3-D region around a grain was used by Brown et al. [32]. The major contribution of their work is that the authors proposed a new value for the Kozeny constant (i.e. 1 instead of 5) to allow for a better agreement of the Kozeny–Carman relationship with their numerical study. It remains however unclear whether this deviation from the original constant is due to the restricted size of the simulation.

In this article the well established idea of a network model [38–43] is extended and newly applied in the field of alloy solidification. The main idea is to represent fluid flow conducts within the semi-solid by a set of geometrical simplified and interconnected channels. Solidification is then included on an individual channel basis, while fluid flow through the represented semi-solid is determined by the flow through the whole channel network.

The advantage of this kind of model is that it allows for investigations which are experimentally not possible and which involves interactions between a lot (i.e. hundredths) of grains at high solid volume fractions. Therefore, the model is suited to investigate the Kozeny–Carman relationship. Furthermore, it is expected that percolation or self induced macro-segregation effects will be revealed with this approach if they exist within solidifying alloys.

2. Model description

The semi-solid state of alloys often consists of solidifying grains within liquid. From a numerical point of view, there are two main approaches to study such semi-solid alloys. On the one hand, it is possible to study development of a few individual grains in detail. Because this involves accurate simulation on the scale of microns and less, the resulting models are called microscopic models. On the other hand, it is possible to average over a large number of grains and study the macroscopic behavior of the semi-solid. With averaging, all conservation equations will be written in terms of liquid or solid volume fractions. Note that the conservation equations are not directly related to the actual microscopic structure.

There exists various ways of coupling microscopic and macroscopic models. But the coupling usually involves assumptions (e.g. restriction to 2-D, no shrinkage) which considerably reduce the complexity of the model. Therefore, all micro–macro models are somehow restricted like the model described below. It relies heavily on a number of assumptions as stated below. However, the model restrictions are chosen in such a way that the interactions of the macroscopic liquid flow and the individual behavior of the grains can be retained. For this reason, this model has the characteristics of a mesoscopic model.

2.1. Basic concept

The basic idea behind the simulation model presented in this article is that the complex structure of the mush, i.e. of the dendritic grains surrounded by the liquid phase, can be represented by a set of interconnected liquid channels. In this paper 2-D networks have been chosen to represent the mush. As shown in Fig. 1 the channel network resembles a distorted padding of a regular hexagonal network.

To create the channel networks a random distribution of grain centers is used. The Voronoi diagram which belongs

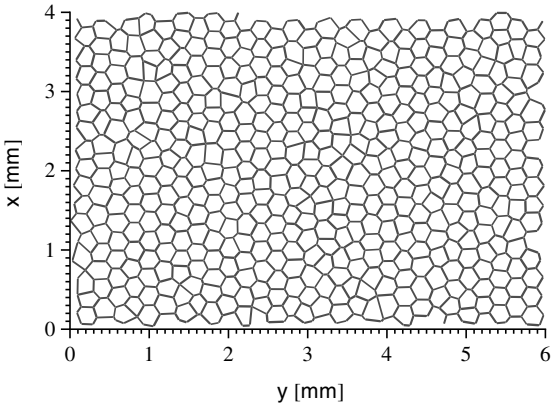

Fig. 1. Liquid channel network.

to the grain centers forms the channel network. Due to the irregular distribution of the grain centers, there exists a certain variation of the channel lengths. If the distance between two grain centers is below a certain threshold, one of the grain centers will be removed and the channel network is adapted accordingly. This last procedure limits the minimal length of a channel.

Dynamical adaptations of the channel widths will account for solidification and melting of grains within the mush. This in turn has an impact on the conductivity of the channels. Liquid pockets of a real mush will undergo many changes before they disappear. It is therefore possible that a representing channel network of an extended model ought to change its structure and especially its connectivity during solidification.

For simplicity reasons it is assumed here that all structural changes will happen only on an individual channel basis. Other kind of structure changes will be explicitly excluded from the model. Furthermore, it is taken, for granted that neither grain centers nor channel junctions will change their positions.

The exact form of the grains the channels represent being unknown, all curvature effects on solidification will be neglected. This also means that no coarsening effects can be included. As a first attempt, the channels are considered to be bounded by parallel planes. Fluid flow within the channels is assumed to be laminar and unidirectional in the main channel direction. Solidification rules are chosen in such a way that a channel solidifies or melts equally on both sides and along its whole length.

The remaining model can be described as follows: if a pressure difference is applied on those channel junctions which serve as inlets and outlets, a fluid flow through the channels will be generated. This flow transports solute and heat. Depending on the temperature and solute concentration of the solid, the convected solute and heat can cause solidification or melting within an individual channel. This in turn might change the temperature and concentration of the effluent fluid flow.

In accordance with this, within every time interval the simulation consists of four parts. Firstly, the flow rates within the whole network are estimated. Secondly, mixing on the channel junctions and within the individual channels determines the amount of convected heat and solute. Thirdly, solidification or melting will determine new channel properties. And finally conduction of heat and solute within the solid is accounted for. Within the simulation all four parts are addressed in turn because they rely on the outcome of each other. In the next section we describe these parts in more detail.

2.2. Fluid flow determination

In order to determine the flow rate within the whole network it is assumed that the overall flow rate through one single channel is proportional to the mean pressure difference of the channel junctions it is connected to, i.e. that

$$Q = K\frac{\Delta p}{L_c}, \tag{2}$$

where Q is the flow rate in the channel, K is the permeability of the channel itself, Δp is the junction pressures difference, and L_c is the channel length.

Since the exact structure of the channels is unknown, the laminar flow within the individual channels is assumed to correspond to the flow between two parallel plates i.e.

$$K = \frac{1}{12}\frac{DW^3}{\eta}. \tag{3}$$

The height of all channels D can be chosen arbitrary, while W is the channel width and the constant η is the viscosity of the channel liquid. For a 2-D simulation this assumption is the most obvious choice. Physically it corresponds more or less to the flow along columnar grains. It is also possible to assume a flow within cylindrical tubes. However, to get a situation corresponding more to the flow around globular grains a network with connections in 3-D is needed. Such a model is at the moment not feasible due to the high computational power it requires.

On the channel junctions mass is conserved. Assuming an incompressible fluid, this allows usage of Eq. (2) to write a system of linear mass balance equations for the whole network. Once the pressures of the inlet and outlet junctions are specified, the system of linear equations can be solved for the unknown pressures on the channel junctions. Finally, the flow rates within the individual channels can be determined with Eq. (2).

A more detailed description of this procedure can be found in Seeburger and Nur [39]. In our simulation however, the system of linear equations often cannot be solved in a direct manner. When solidification proceeds, some channels will soon have a reduced width, while other channels tend to stay open. The effect is a huge difference between the smallest and largest channel permeability K. This in turn leads to an ill conditioned system of linear equations.

To avoid numerical instabilities permeability values below a certain threshold are set equal to zero and the resulting equation system is divided into linear independent parts if possible. For this division a coloring algorithm showed to be useful. It assigns all channel junctions which are connected to each other by a nonzero permeability channel to the same color. Each cluster of colored junctions represents one independent part of the whole system of equations.

2.3. Solidification and melting

Solidification and melting within a channel can occur if either the predefined channel liquid temperature and/or the liquid solute concentration of the channel changes. The cause for this can be either convection from inlets or from upstream channels or conduction and diffusion across the network.

In order to keep the description of solidification simple each channel is described by one single element. The channel elements are characterized by a uniform channel concentration, temperature and channel width. When the simulation starts the initial liquid concentration and temperature are chosen to correspond to a point of the liquidus within the phase diagram. The same holds for the inlet flow as well.

During solidification all three parameters describing the channel, i.e. liquid concentration, temperature and width can change. However, in the noneutectic regime the liquid at the interface will retain a concentration and temperature which still belongs to the liquidus. Therefore, solidification only changes the location on the liquidus while altering the channel width.

For the determination of solidification a linear phase diagram is used. This has two advantages. Firstly, determination of the liquidus temperature given the liquid concentration and vice versa is straight forward. Secondly, when two liquids with both corresponding points on the liquidus are completely mixed, the resulting liquid will still correspond to a point on the liquidus.

This strong coupling of the system to the liquidus permits approximation of the solidification rate in three steps. The first and most difficult step is the prediction of the new temperature of the liquid at the end of the considered time interval. This is followed by the determination of the liquid solute concentration which in turn is used for the estimate of the new channel width. All three steps are set up to be applicable on individual channels. We assume that during a step the behavior of the other channels do not interfere.

At first the liquid temperature within a channel T_0 is likely to be different from the temperature of its surrounding region. During equilibration of heat, the temperature changes and solidification or melting will be induced. If time permits, a final averaged temperature T_∞ will be reached. In the simulation this temperature is approximated by an area weighted mean temperature of both neighboring elements of the channel.

How the initial temperature T_0 changes to T_∞ is strongly related to the development of the micro-structure within the channel. On the level of a mesoscopic model it is not attained to spend a lot of computational effort in its simulation. Therefore it is assumed that the development of temperature can be reasonably described by an exponential function of the form

$$T = T_\infty + (T_0 - T_\infty)\mathrm{e}^{-\frac{\dot{T}(t=0)}{T_0 - T_\infty}t}. \tag{4}$$

In this equation, the liquid temperature of the channel is T. Its derivative $\dot{T}$ has to be taken at time $t = 0$ and is approximated by

$$\dot{T}(t=0) = -\frac{k_\mathrm{s}\left(\frac{T_0 - T_1}{d_1} + \frac{T_0 - T_2}{d_2} - 2v_i L\right)}{\rho_\mathrm{l} C_{p\mathrm{l}} W_0}. \tag{5}$$

In this equation, which is derived from heat conservation, k_s is the solid conductivity, $C_{p\mathrm{l}}$ the specific heat of the liquid, ρ_l the density of the liquid and L is the latent heat of fusion. Apart from the material constants, the initial channel width W_0, the interface velocity v_i, the temperatures of the neighboring elements T_1, T_2 and the distances to its grain centers d_1, d_2 have to be known.

The solid–liquid interface velocity of both channel walls is assumed to be the same. Otherwise dislocation of the channel can occur. While all parameters in Eq. (5) are given by boundary conditions or follow directly from the simulation, the interface velocity is not. With Eq. (5) a new channel width can be predicted and in consequence a new corresponding interface velocity can be determined. If the time duration of solidification is short enough, this determined velocity should equal to the velocity used in Eq. (5) itself. In the model the difference of both velocities is minimized using a Newton method and very short time steps.

Once the best velocity is found, Eq. (4) is applied for the whole duration of one iteration and a new liquid temperature T_l at the end of it is determined. The corresponding solute concentration within the channel C_l is then given by the relation describing the liquidus

$$C_\mathrm{l} = \frac{T_\mathrm{f} - T_\mathrm{l}}{m}, \tag{6}$$

where T_f is the melting temperature of the pure solvent and m is the slope of the liquidus (Table 1).

Finally, the prediction of solidification is terminated by estimating a new channel width W_l using Scheil–Gulliver equation

$$W_\mathrm{l} = W_0\left(\frac{C_\mathrm{l}}{C_0}\right)^{(k-1)} \tag{7}$$

with partition coefficient k. In principle all similar equations, such as those incorporating back diffusion, can be used here.

Within the eutectic regime the growth rate is assumed to depend linearly on the amount of undercooling from the eutectic temperature T_eut, i.e.

$$v_i = \beta(T_\mathrm{eut} - T_0). \tag{8}$$

Table 1
Material constants used in the simulation

Melting temperature of Al, T_f	933.6 K
Eutectic composition, T_e	33.1 wt%
Partition coefficient, k	0.16
Liquidus slope, m	−3.7 K/wt%
Diffusion coefficient (in solid), D_s	1.5×10^{-13} m^2/s
Thermal conductivity (in solid), k_s	120.7 W/K m
Latent heat of fusion, L	3.9×10^5 J/m^3
Specific heat of solid, $C_{p\mathrm{s}}$	958.0 J/kg K
Specific heat of liquid, $C_{p\mathrm{l}}$	1054.0 J/kg K
Viscosity (of liquid), η	0.0023 Ns/m^2
Solid density, ρ_s	2750.0 kg/m^3
Liquid density, ρ_l	2460.0 kg/m^3
Kinetic coefficient, β	0.1 m/s K

This is only a very crude estimate but it allows choosing an adequate kinetic coefficient β. In this way a qualitative estimate of experimental observed increase or decrease of the solidification rate of eutectics can be made.

2.4. Mixing

At the channel junctions total mixing of the influent liquids is assumed. The model will use for every channel junction the liquid Temperature T_l and solute concentration C_l of each adjacent channel with an inflowing liquid. The temperature of the mixed fluid at a channel junction is determined by

$$\overline{T} = \frac{\sum_i T_i V_i}{\sum_i V_i}. \tag{9}$$

It is the mean of all temperatures T_i of the influent liquids mixing within the same junction. The temperatures are weighted with the corresponding volume of influent liquids V_i that leaves channel i during the duration of one simulation interval. The solute concentration is averaged in the same way.

Due to mass conservation, the same amount of liquid flowing into a channel junction has to flow out of it. This influent liquid will mix within the remnant liquid of the channel it flows into. The model assumes that this mixing is complete. The new liquid temperature and solute concentration due to the mixing is determined just before solidification is considered.

2.5. Conduction and diffusion

The spread of heat and solute within the whole mush by conduction and diffusion is determined using an ordinary finite volume method. The meshing of the network is shown in Fig. 2. During the simulation the network will be adapted. The size of the channel elements are then changed in accordance to the channel widths. Neighboring elements of the channel elements are eliminated or introduced depending on the new grain extend. This all is done minding mass and heat conservation.

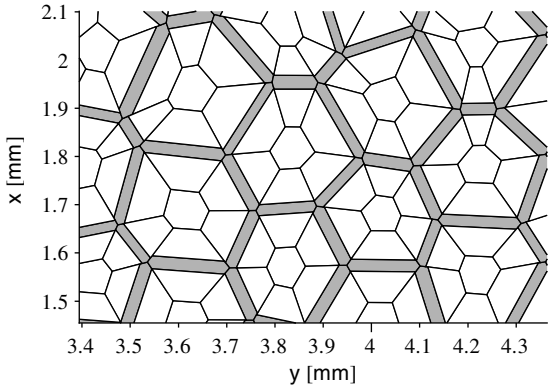

Fig. 2. Magnified detail of the liquid channel network (gray) as shown in Fig. 1. In addition the meshing of the grains is shown.

3. Observations and numerical results

The described network model has been used to determine the behavior of a Al–Cu mush of uniform temperature upon inflow of a slightly higher temperature. For this purpose the network structure shown in Fig. 1 which contains 559 grains and 1465 channels was created. It represents a mush with extend of about 4 mm by 6 mm. The mean grain size was chosen to be around 200 μm. The initial channel widths have been chosen to be normal distributed with mean width of 12.5 μm and a standard deviation of 2 μm.

Initially the whole network array has a uniform temperature of 880 K and a solute concentration which corresponds to this temperature in accordance to the phase diagram. The bottom junctions of the network are considered to be inlets while a row of junctions at the top of the network serve as outlets. A fluid flow from the inlets to the outlets is created by applying a pressure difference of 10,900 Pa. The inflowing fluid had a fixed temperature of 885 K during the whole simulation. Its corresponding solute concentration was determined by the liquidus and was around 14.5 wt% Cu.

During the whole simulated duration of 0.132 s comprising 1600 time iterations, a temperature of 880 K was imposed on the top most grain centers of the network. On all other boundaries conditions were chosen such that no heat nor solute is lost by conduction or diffusion. Of course convection was allowed to transport heat and solute into the system at the inlets. Furthermore, it was made sure that no solute conduction occurred at the top of the network.

The system behaved as expected during the simulation. First, through convection a lot of heat is transported to the bottom part of the network. The channel liquid thereby cools down while heat is conducted into the solid part. This cooling induces solidification at the channel walls. The solidification in turn means that the channels become narrow and convection is greatly reduced. However, the dimensionless Péclet number is small (i.e. below 0.2) which means that conduction of heat is much faster than convection. What follows is that temperature becomes nearly equalized over the whole width of the network and heat will be transported mainly by conduction.

It is interesting to see, that during the whole simulation the system behaves well balanced. That means there seems to occur neither self induced nor random effects. Speculations predicting that some channels might start to widen dramatically while its neighbor have to close seems to be unfounded. The effect of wormhole formation was neither found anywhere.

The influence of a random channel width distribution is clearly visible at the beginning of the simulation. However, when the bottom channels decrease in width convection

will soon be predominated by heat conduction and the initial widths distribution will play a minor role.

4. Discussion

As can be seen from Fig. 3 permeability is within the range of the measured values. Permeability decreases at first slowly due to the fact that it takes some time till enough liquid of augmented temperature is convected into the lower channels of the network. Once heat can be extracted from the channel liquid solidification becomes increased and permeability declines rapidly. In the end permeability tends to decrease slowly because of the reduced amount of temperature augmented liquid inflow. The channels near the inlets have then become too narrow.

Using expression (1) it is possible to determine the development of the Kozeny factor k_c (see Fig. 4). At the beginning k_c is nearly constant and its value is about the expected Kozeny constant of 5. Later on the k_c rises due to the rapid decrease of permeability while the liquid fraction f_l decreases and the specific surface S_S increases slowly as can see in Figs. 5 and 6, respectively. The specific surface S_S, i.e. the length of the solid–liquid interface per array of solid, first decreases even though the whole interface length increases. This is caused by the assumed channel geometry.

The variation of the Kozeny factor indicates a deviation from Kozeny–Carman relationship. This can be clearly seen in Fig. 7. In this figure the experimental measured dimensionless permeability values and the expected development as predicted by the Kozeny–Carman relationship are compared with the values derived from simulation. The dimensionless permeability in the simulation decreases while the liquid volume fraction within the network seems to remain nearly constant. Further investigation revealed that only the lowest channels near the inlets experience enough solidification to narrow considerably. The narrowing of these channels however does not influence the liquid fraction remarkably.

If only the lower part of the network gets influenced by the inflow of the temperature augmented liquid, it is interesting to consider a more localized permeability. Fig. 8 shows that within the considered model it is statistical pos-

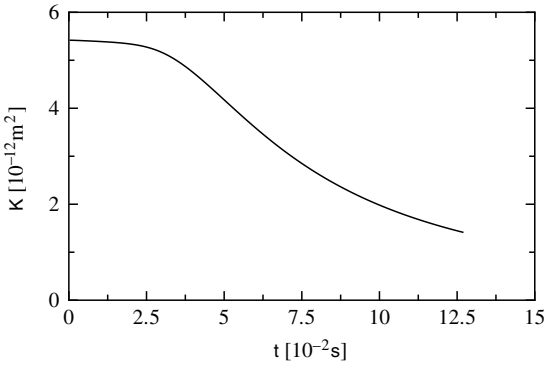

Fig. 3. Development of permeability within the channel network.

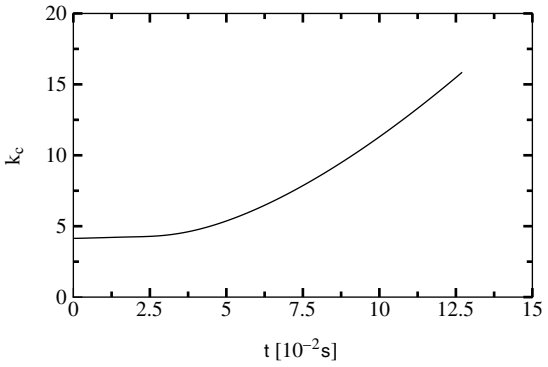

Fig. 4. Development of the Kozeny factor.

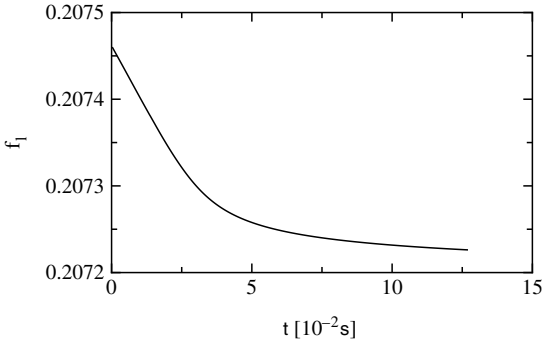

Fig. 5. Decrease of the volume fraction of liquid.

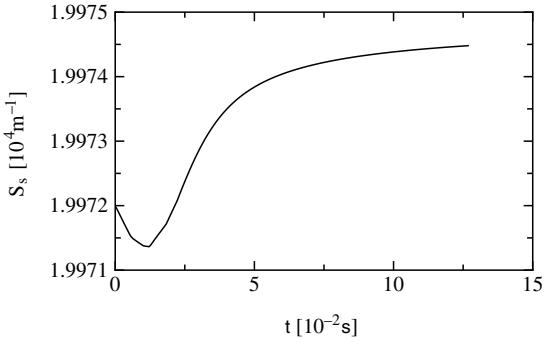

Fig. 6. Increase of the specific surface.

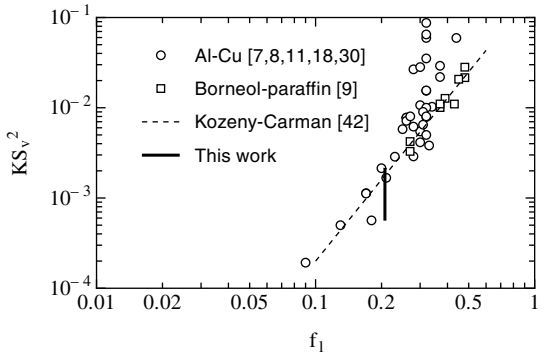

Fig. 7. Dependence of the dimensionless permeability on the liquid volume fraction.

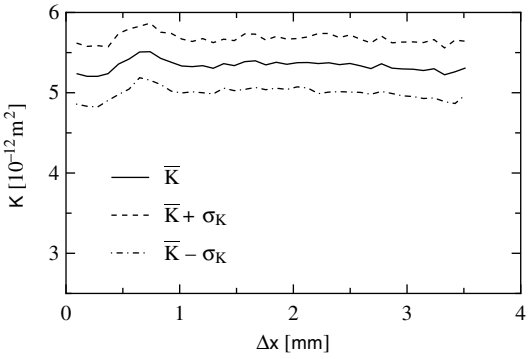

Fig. 8. Influence of the region length in x-direction on the determination of a localized permeability. The regions are localized around the center of the network and have width of 1.5 mm (in y-direction).

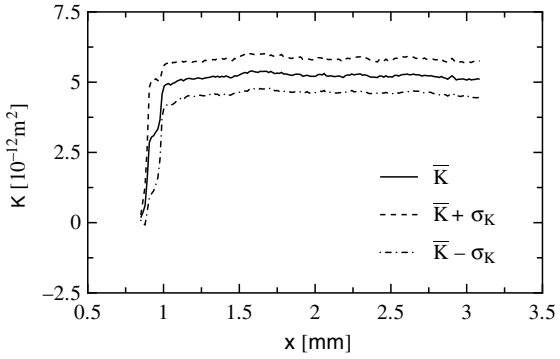

Fig. 9. Averaged permeability in x-direction at 0.088 s. The regions used to determine permeability had a length of 1 mm in x-direction and 1.5 mm in the other direction.

sible to consider Darcy's law on localized regions with a minimal length of about 1 mm. Using regions of this minimal length the permeability within the network has a typical profile as shown in Fig. 9. Permeability remains nearly constant during the whole simulation in nearly the whole network but for the bottom part. Within the bottom part of about 200 μm length flow gets remarkably hampered. Only within this bottom part application of the Kozeny–Carman relationship makes sense.

Though the considered situation in this article is special, the clear importance of small regions within the mush indicates that only slight in-homogenization of measured samples or of the temperature distribution within, can have dramatic effects. All measurements included in Fig. 7 use relatively large sized samples. It therefore might be that this is a reason among others for the wide spread of the measured values.

As it is possible that the already mentioned relative stability of the network depends on the applied pressure and on the initial channel width distribution, some additional simulations with higher pressure drops and wider width distributions were carried out. The results show no anomaly. In Fig. 10 the influence of the variation of the width distribution on permeability is shown. As expected a wider

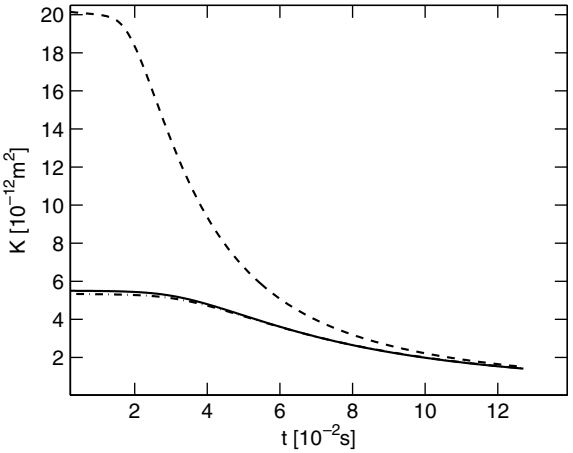

Fig. 10. Influence of the initial width distribution of the liquid channels on permeability. The solid line represent a network with initial width of 12.5 ± 2 μm. The dash-dotted line corresponds to an initial width of 12.5 ± 6 μm and the dotted line is the result of initial width of 20 ± 15 μm.

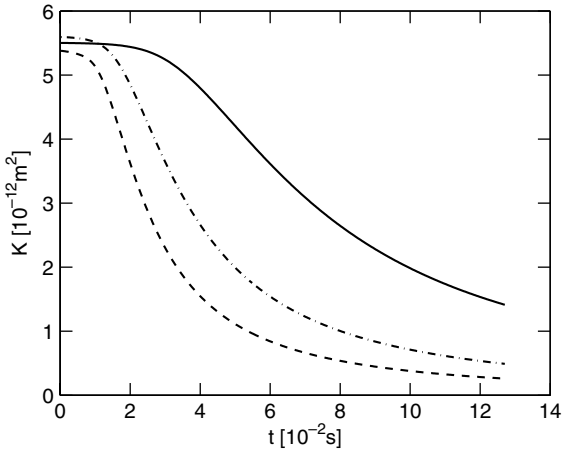

Fig. 11. Influence of the applied pressure difference on permeability. The solid line was determined with a pressure difference of 10.9 kPa, the dash-dotted line corresponds to 21.8 kPa and the dotted line was determined with a difference of 32.7 kPa. The initial random widths of the liquid channels was for each simulation generated anew (with 12.5 ± 2 μm).

variation of the initial liquid channel widths has only a marginal effect on permeability, while the mean width influences permeability directly.

Some results of simulations with higher pressure differences are shown in Fig. 11. A higher difference of the applied pressure leads to a faster decrease of the permeability. The reason is that a higher pressure difference increases the amount inflowing warm fluid which will solidify upon cooling.

5. Conclusions

Above description shows that it is possible to extend a network model for the flow simulation of liquid within semi-solid Al-alloys. The network model can be coupled to an ordinary finite volume method which simulates the

conduction of heat and diffusion of solute within the solid. Though many introduced restrictions, the resulting dynamic mesoscopic 2-D model has been shown to be able to simulate the fluid flow within a solidifying mush adequately. Especially the values for permeability and for the Kozeny constant are comparable with measured values.

The extended model was applied to simulate the inflow of liquid with a slightly increased temperature into a mushy zone of uniform temperature. It was shown that no self induced effects like wormhole formation occur upon this inflow. The whole system remains rather stable. As expected the inflow just induces an increase of solidification at the inlet side of the mush. A random distribution of the initial channel widths is visible to a certain extend before its effect disappears completely.

Finally, it is indicated that the behavior of small regions within relative large samples might lead to a spread of measured permeability values. This indication is guided by the observation that the overall permeability can heavily depend on the alteration of the morphology within a comparable small region.

Acknowledgements

The authors thank A.J. Dammers who initiated this research. The discussions with D.G. Eskin are gratefully acknowledged.

References

[1] M.C. Flemings, G.E. Nereo, Trans. Metall. Soc. AIME 239 (1967) 1449.
[2] M.C. Schneider, C. Beckermann, Int. J. Heat Mass Transfer 38 (1995) 3455.
[3] J. Ni, F.P. Incropera, Int. J. Heat Mass Transfer 38 (1995) 1271.
[4] B. Goyeau, T. Benihaddadene, D. Gobin, M. Quintard, Transport Porous Media 28 (1997) 19.
[5] B.C.H. Venneker, L. Katgerman, J. Light Met. 2 (2002) 149.
[6] R.J. Feller, C. Beckermann, Metall. Mater. Trans. B 28B (1997) 1165.
[7] D.R. Poirier, G.H. Geiger, Transport Phenomena in Materials Processing, TMS, Warrendale, 1994, p. 90.
[8] D.R. Poirier, S. Ganesan, Mater. Sci. Eng. A157 (1992) 113.
[9] A.J. Duncan, Q. Han, S. Viswanathan, Metall. Mater. Trans. B 30B (1999) 745.
[10] K. Murakami, T. Okamoto, Acta Metall. 32 (1984) 1741.
[11] T.S. Piwonka, M.C. Flemings, Trans. Metall. Soc. AIME 236 (1966) 1157.
[12] J.W.K van Boggelen, D.G. Eskin, L. Katgerman, Light Met. (2003) 759.
[13] B. Goyeau, T. Benihaddadene, D. Gobin, M. Quintard, Metall. Mater. Trans. B 30B (1999) 613.
[14] P. Bousquet-Melou, B. Goyeau, M. Quintard, F. Fichot, D. Gobin, Int. J. Heat Mass Transfer 45 (2002) 3651.
[15] A. Neculae, B. Goyeau, M. Quintard, D. Gobin, Mater. Sci. Eng. A323 (2002) 367.
[16] H.-J. Diepers, C. Beckermann, I. Steinbach, Acta Mater. 47 (1999) 3663.
[17] C. Beckermann, H.-J. Diepers, I. Steinbach, A. Karma, X. Tong, J. Comp. Phys. 154 (1999) 468.
[18] J.-H. Jeong, N. Goldenfeld, J.A. Dantzig, Phys. Rev. E 64 (2001) 041602-1.
[19] Ø. Nielsen, L. Arnberg, Metall. Mater. Trans. A 31A (2000) 3149.
[20] D.R. Poirier, Metall. Trans. B 18B (1987) 245.
[21] S. Viswanathan, A.J. Duncan, A.S. Sabau, Q. Han, Modeling of Casting, Welding and Advanced Solidification Processes VIII, 1998, p. 849.
[22] P.M. Adler, Porous Media: Geometry and Transports, Butterworth-Heinemann, Stoneham, 1992, p. 159.
[23] F.A.L. Dullien, Porous Media: Fluid Transport and Pore Structure, Academic Press, San Diego, 1992, p. 240.
[24] M. Sahimi, Flow and Transport in Porous Media and Fractured Rock; From Classical Methods to Modern Approaches, VCH, Weinheim, 1995, p. 400.
[25] F.A.L. Dullien, Porous Media: Fluid Transport and Pore Structure, Academic Press, San Diego, 1992, p. 253.
[26] M.S. Bhat, D.R. Poirier, J.C. Heinrich, Metall. Mater. Trans. B 26B (1995) 1091.
[27] M.S. Bhat, D.R. Poirier, J.C. Heinrich, Metall. Mater. Trans. B 26B (1995) 1049.
[28] S. Ganesan, C.L. Chan, D.R. Poirier, Mater. Sci. Eng. A151 (1992) 97.
[29] J.C. Heinrich, D.R. Poirier, D.F. Nagelhout, Comp. Meth. Appl. Mech. Eng. 133 (1996) 79.
[30] M.S. Bhat, D.R. Poirier, J.C. Heinrich, D. Nagelhout, Scripta Metall. Mater. 31 (1994) 339.
[31] D. Bernard, L. Salvo, Ø. Nielsen, Modeling of Casting, Welding and Advanced Solidification Processes X, 2003, p. 175.
[32] S.G.R. Brown, J.A. Spittle, D.J. Jarvis, R. Walden-Bevan, Acta Mater. 50 (2002) 1559.
[33] C.Y. Wang, C. Beckermann, Metall. Trans. A 24A (1993) 2787.
[34] C.Y. Wang, S. Ahuja, C. Beckermann, H.C. de Groh III, Metall. Mater. Trans. B 26B (1995) 111.
[35] H. Laux, personal communications, 2001.
[36] H. Laux, Ø. Nielsen, in: Proceedings of 2002 IMECE, p. IMECE2002-32884.
[37] J. Ni, C. Beckermann, Metall. Trans. B 22B (1991) 349.
[38] F.A.L. Dullien, Porous Media: Fluid Transport and Pore Structure, Academic Press, San Diego, 1992, p. 192.
[39] D.A. Seeburger, A. Nur, J. Geophys. Res. 89 (1984) 527.
[40] M.L. Hoefner, H.S. Fogler, AIChE J. 34 (1988) 45.
[41] Y. Bernabé, C. Bruderer, J. Geophys. Res. 103 (1998) 513.
[42] Ch. Pan, M. Hilpert, C.T. Miller, Phys. Rev. E 64 (2001) 066702-1.
[43] P.C. Carman, Flow of Gasses Through Porous Media, Butterworth Scientific, London, 1956.